RESEARCH ARTICLE

Figures and figure supplements

Formation of multinucleated osteoclasts depends on an oxidized species of cell surface-associated La protein

Evgenia Leikina and Jarred M Whitlock *et al*.

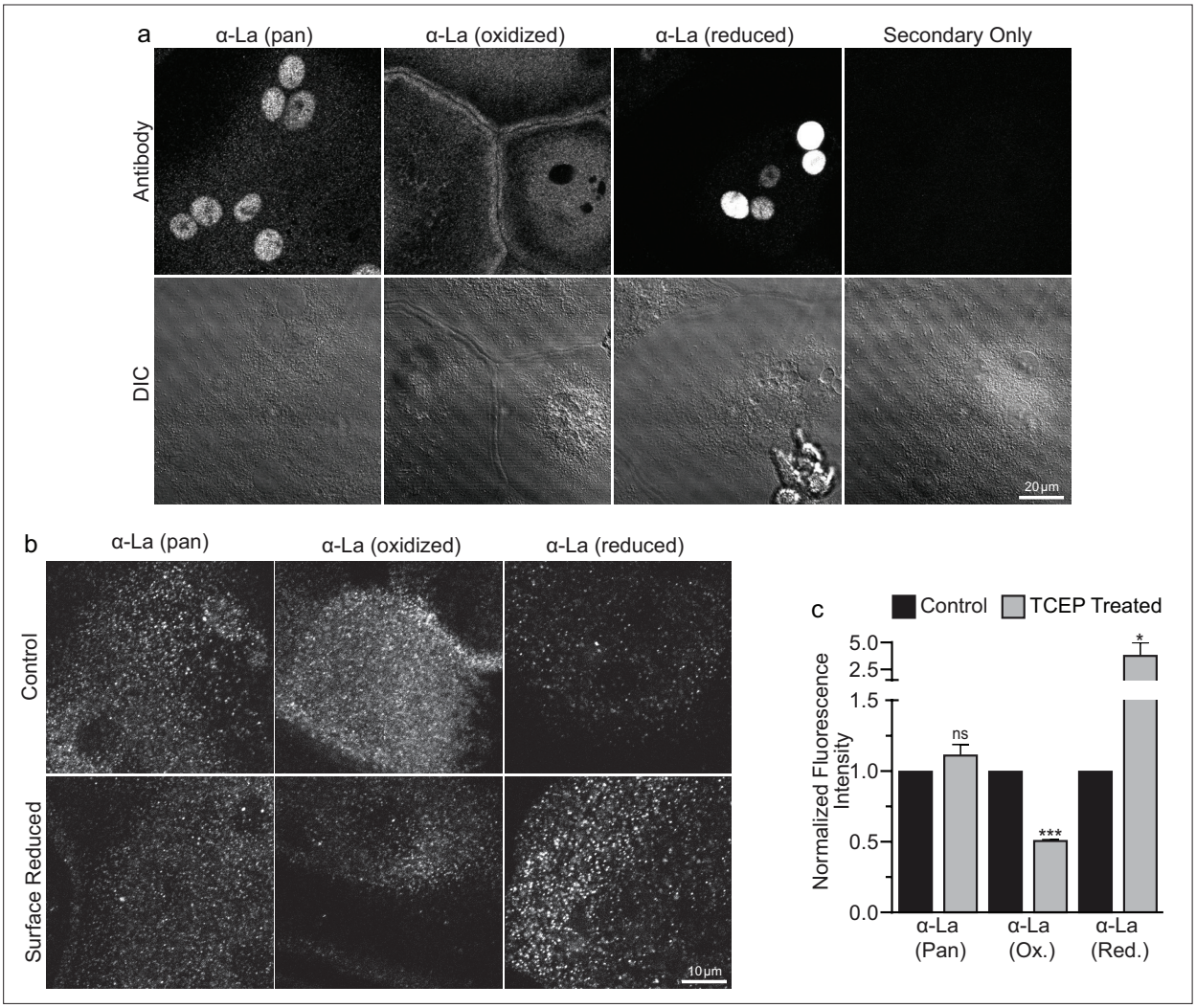

Figure 1. Oxidized La decorates the surface of osteoclasts during multinucleation. (**a**) Representative immunofluorescence (top) and differential interference contrast (DIC, bottom) confocal micrographs of permeabilized primary human osteoclasts. La localization was visualized via a general α-La antibody (Pan), an α-La antibody that recognizes oxidized La, or an α-La antibody thar recognizes reduced La (described and validated in ***Berndt et al., 2021b***). (**b**) Representative immunofluorescence confocal micrographs of primary human osteoclasts stained with the antibodies described in (**a**) under non-permeabilized conditions to visualize surface La. Surface La pools were visualized for the untreated cells (control) and for cells treated with the membrane-impermeable reducing reagent TCAP. (**c**) Quantification of (**b**) (n = 3) (p = 0.13, 0.0001, and 0.03, respectively). Statistical significance evaluated via paired *t*-test. * = $p < 0.05$. *** ≤ $p < 0.0001$. Data are presented as mean values +/- SEM.

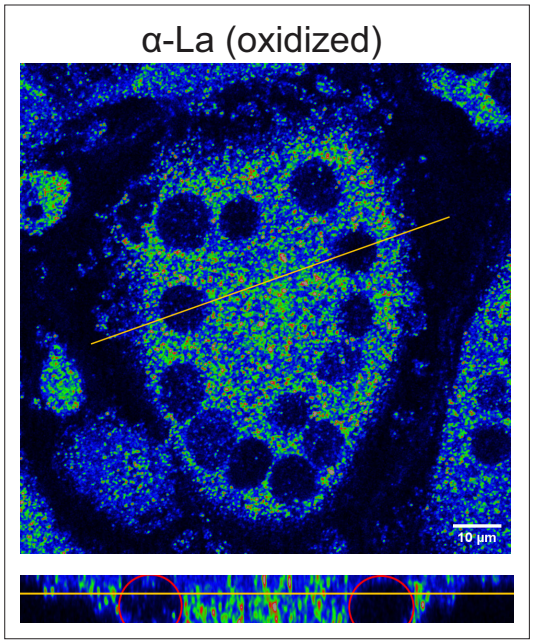

Figure 1—figure supplement 1. Oxidized La is found in the cytosol. 3D stack image depicting the cytosolic localization of oxidized LA. Top – XY-slice slightly below the equatorial plane of a permeabilized multinucleated osteoclast (3 days post-receptor activator of NF-kappaB ligand [RANKL] application) stained with an α-La antibody that recognizes oxidized La. 3D stack of this representative cell was acquired with 0.22 mm step interval. Bottom – Z-slice through the orange line on the top panel. Red ellipses show the approximate outlines of two nuclei in the slice, and the orange line shows the location of the XY-slice shown on top.

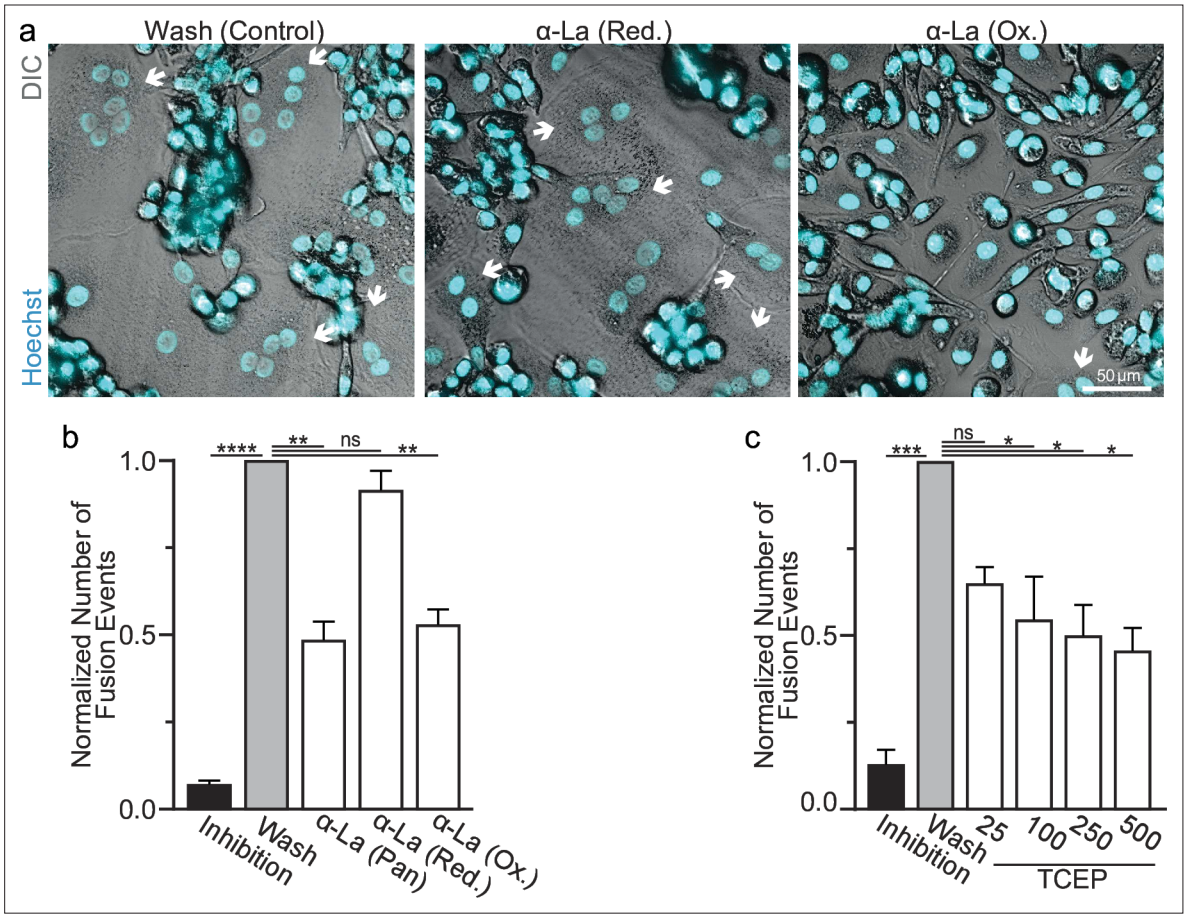

Figure 2. Oxidized La promotes osteoclast membrane fusion. (**a**) Representative fluorescence and differential interference contrast (DIC) confocal micrographs of primary human osteoclasts following synchronized cell–cell fusion where hemifusion inhibitor was left (Inhibition), removed (Wash), or removed but the α-La antibodies indicated were simultaneously added. Cyan = Hoechst arrows = multinucleated osteoclasts. (**b**) Quantification of (**a**) (*n* = 5) (p = <0.0001, 0.0019, 0.44, and 0.0038, respectively). (**c**) Quantification of synchronized primary human osteoclast fusion events under control conditions or conditions where surface proteins are reduced (Tris (2-carboxyethyl) phosphine, TCEP). Osteoclast fusion was synchronized by reversibly inhibiting cell–cell fusion using the membrane fusion inhibitor lysophosphatidylcholine (LPC). Inhibition = LPC applied and not removed, Wash = LPC applied and removed to allow synchronized fusion, TCEP = same as Wash with the addition of TCEP before LPC removal (n = 4, except 25 where n = 2) (p = 0.0005, 0.36, 0.02, 0.016, and 0.013, respectively). Statistical significance evaluated via paired one-way analysis of variance (ANOVA) with Holm–Sidak correction. * = p < 0.05, ** = <0.01, *** = p < 0.001, ***** ≤ p < 0.0001. Data are presented as mean values +/- SEM.

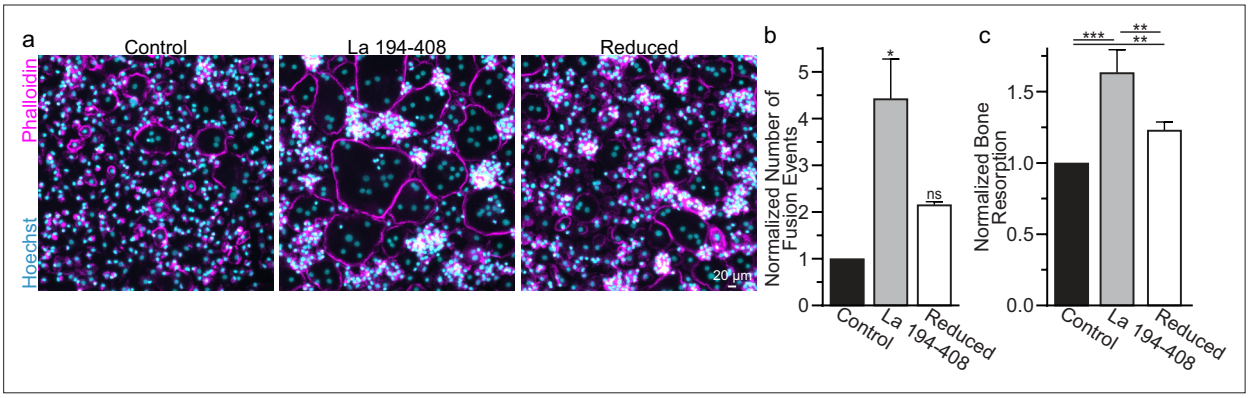

Figure 3. Surface La's oxidation is functionally important for the formation and function of osteoclasts. (**a**) Representative fluorescence images of primary human osteoclast multinucleation following addition of control La 194–408 vs La 194–408 where cysteine residues were reduced by Tris (2-carboxyethyl) phosphine (TCEP) and then blocked by iodoacetamide treatments. Cyan = Hoechst. Magenta = phalloidin. (**b**) Quantification of osteoclast fusion events in (**a**) (*n* = 3) (p = 0.029 and 0.44, respectively). Statistical significance evaluated via paired Friedman test with Dunn's correction. (**c**) Quantification of in vitro resorptive function in conditions described in (**a**) (n = 4) (p = 0.0001, 0.009, and 0.001, respectively). Statistical significance evaluated via paired one-way analysis of variance (ANOVA) with Holm–Sidak correction. * = p < 0.05, ** = <0.01, *** = p < 0.001. Data are presented as mean values +/- SEM.

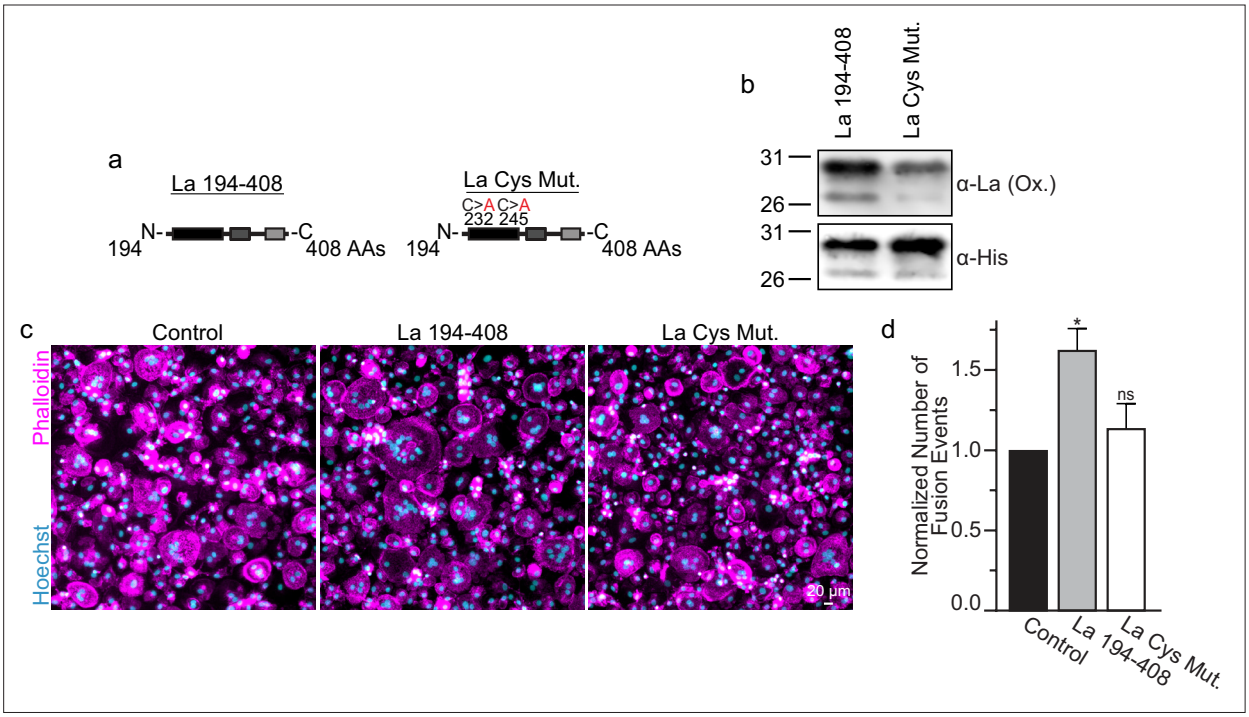

Figure 4. La 194–408 cysteine residues are critical for promoting osteoclast fusion. (**a**) Cartoons illustrating the domain structure of La's C-terminal half and the location of its two cysteines. (**b**) Representative Western Blots depicting La C-terminal half and cystine mutant. (**c**) Representative immunofluorescence micrographs of fusing primary human osteoclasts under control conditions or treated with La 194–408 or cysteine mutant La 194–408. (**d**) Quantification of the number of fusion events observed in (**c**) (n = 4) (p = 0.046 and 0.62, respectively). Statistical significance evaluated via paired one-way analysis of variance (ANOVA) with Dunnett correction. * = $p < 0.05$. Data are presented as mean values +/- SEM.

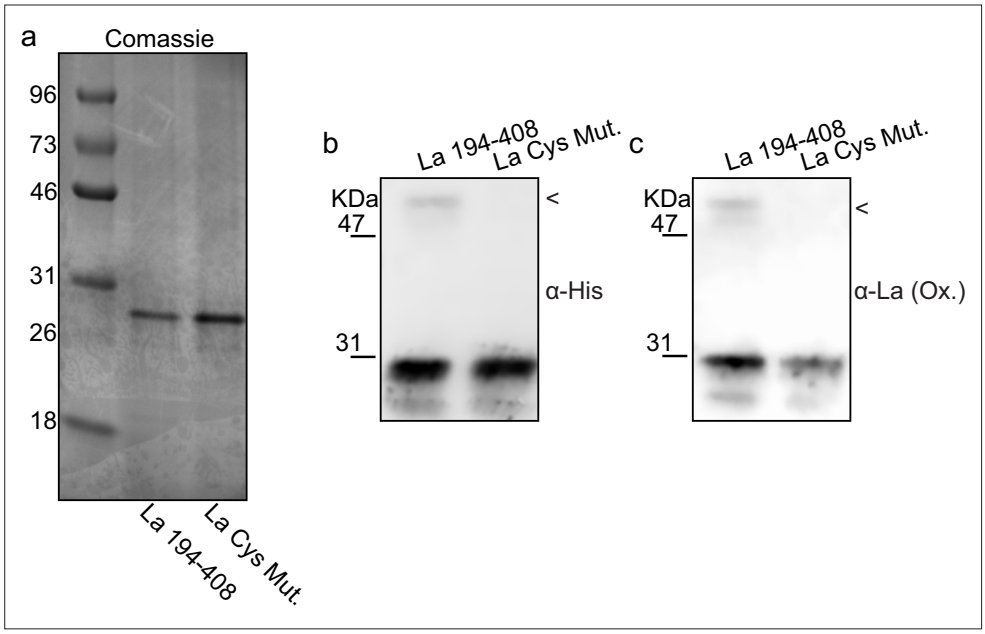

Figure 4—figure supplement 1. La C-terminal half and cysteine mutant purification. (**a**) A gray-scale image of La 194–408 or cysteine mutant La 194–408 separated via polyacrylamide gel electrophoresis and visualized using Coomassie staining. Representative Western Blots depicting La C-terminal half and cysteine mutant recognized by α-6xhis (**b**) or α-La (ox.) α-6xhis (**c**). < denotes the migration of La 194–408 as a dimer.

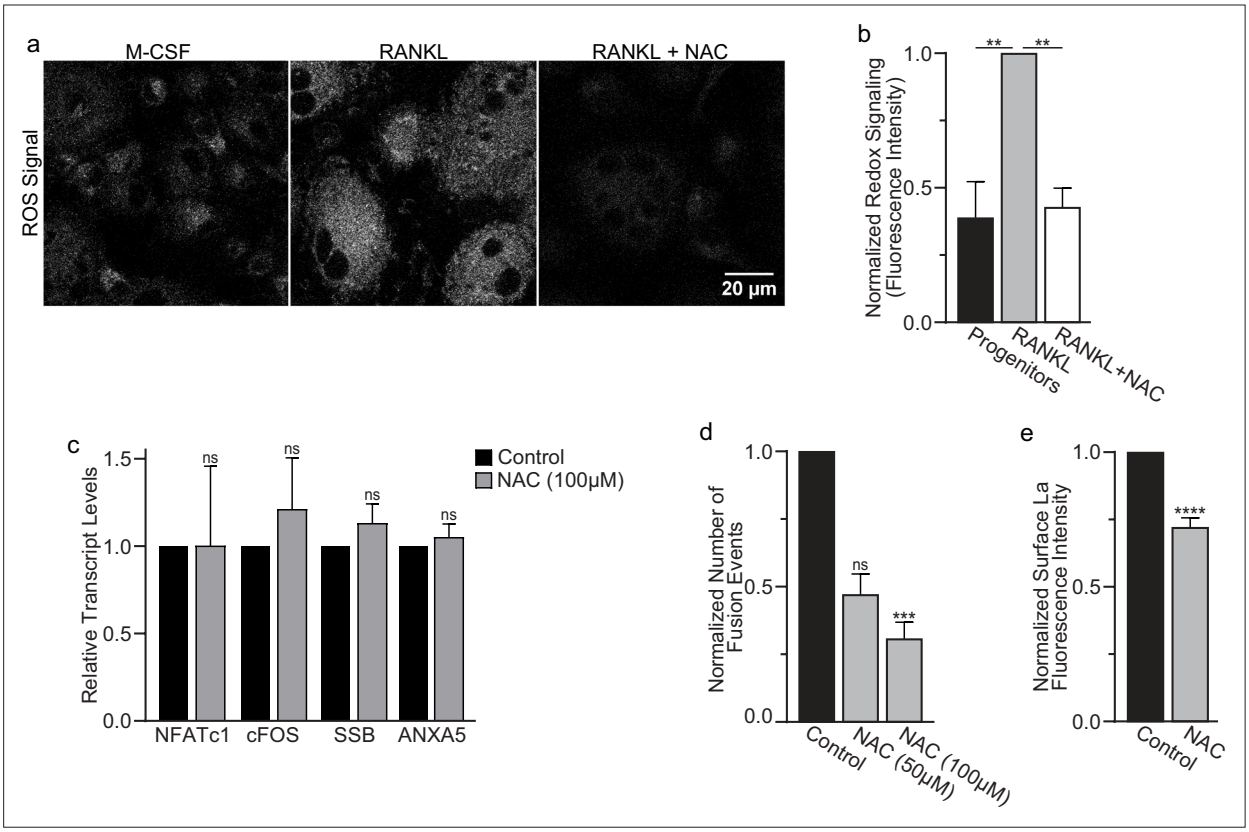

Figure 5. Reactive oxygen species (ROS) promotes oxidized La surface trafficking and osteoclast fusion. (**a**) Representative confocal micrographs of ROS signal in primary human osteoclasts precursors under conditions lacking receptor activator of NF-kappaB ligand (RANKL), following 16 hr of RANKL application, or following 16 and 1 hr 100 µM *N*-acetylcysteine (NAC) treatment (gray = CellRox Dye). (**b**) Quantification of ROS signaling in osteoclast progenitors, committed osteoclasts, or committed osteoclasts treated with the membrane-permeable reducing reagent NAC (n = 2, 4, and 3, respectively) (p = 0.004 and 0.0043, respectively). Statistical significance evaluated via paired one-way analysis of variance (ANOVA) with Holm–Sidak correction. (**c**) qPCR quantification of osteoclastogenesis markers (*NFATc1* and *cFOS*), La transcript (*SSB*), and annexin A5 (*ANXA5*). Expression evaluated in comparison to *GAPDH* (n = 4) (p = 0.50, 0.69, 0.32, and 0.45, respectively). Statistical significance evaluated via paired *t*-test. (**d**) Quantification of the number of fusion events observed between human osteoclasts in control conditions or conditions where fusion was inhibited via NAC treatment (n = 6) (p = 0.057 and 0.019, respectfully). Statistical significance evaluated via paired one-way ANOVA with Holm–Sidak correction. (**e**) Quantification of La surface staining of non-permeabilized cells with pan α-La antibodies at day 3 post-RANKL application without or with 50–100 µM NAC added at day 1 post-RANKL application (n = 9) (p = <0.0001). Statistical significance evaluated via paired *t*-test. ** = <0.01, *** = p < 0.001 ***** ≤ p < 0.0001. Data are presented as mean values +/- SEM.

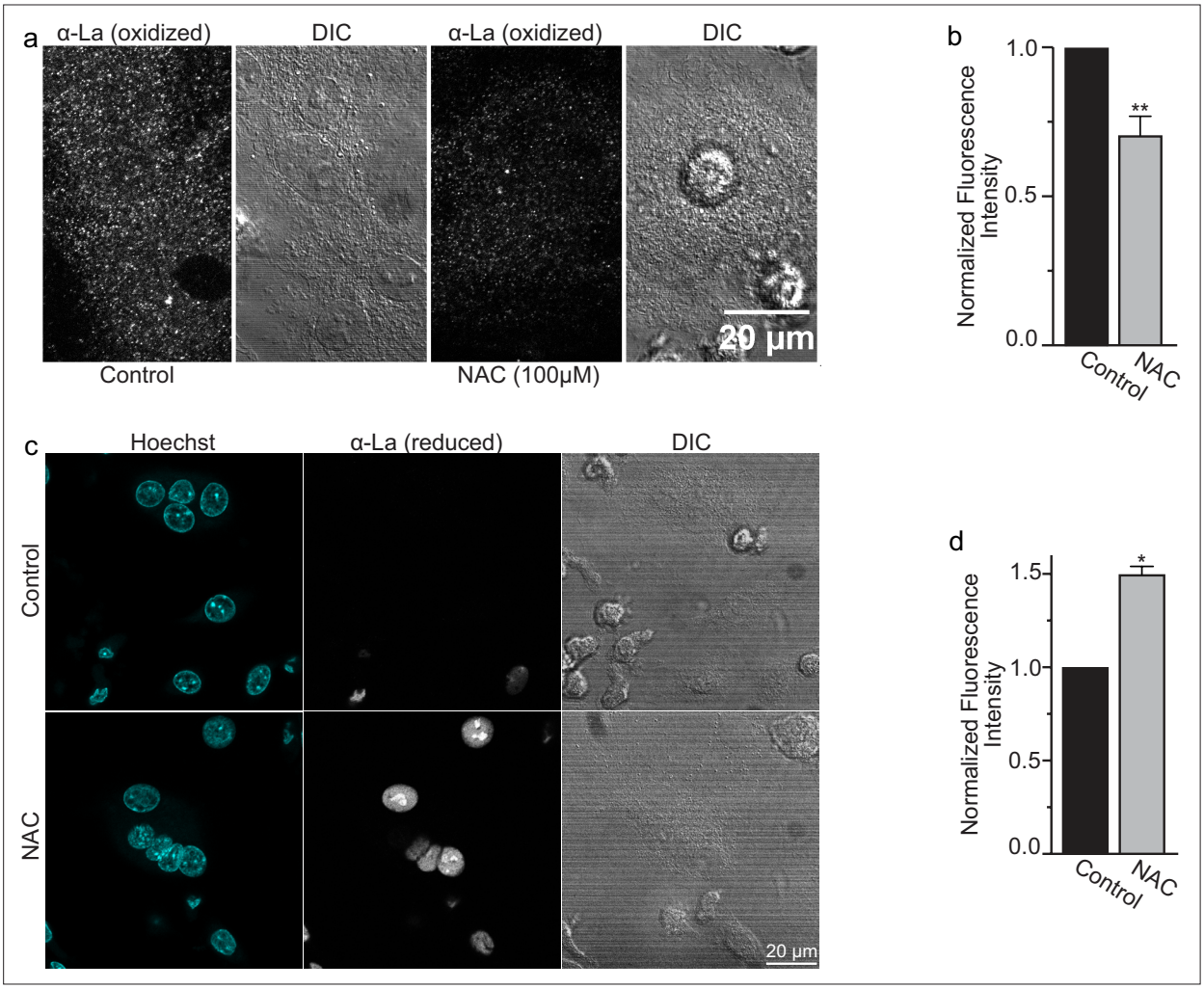

Figure 5—figure supplement 1. *N*-Acetylcysteine (NAC) inhibits redox shift from reduced to oxidized species of intracellular La. (**a**) Fluorescence microscopy and differential interference contrast (DIC) images of permeabilized osteoclasts treated or not treated (control) with 100 mm (1 hr) NAC and stained with an α-La antibody that recognizes oxidized La at 3 days post-receptor activator of NF-kappaB ligand (RANKL) application. (**b**) Quantification of (**a**) (n = 5) (p = 0.009). (**c**) Fluorescence microscopy and DIC images of permeabilized osteoclasts treated or not treated (control) with 100 mm (1 hr) NAC and stained with an α-La antibody that recognizes reduced La at 3 days post-RANKL application. (**d**) Quantification of (**c**) (*n* = 2) (p = 0.04). Statistical significance evaluated via paired *t*-test. * = p < 0.05, ** = <0.01. Data are presented as mean values +/- SEM.

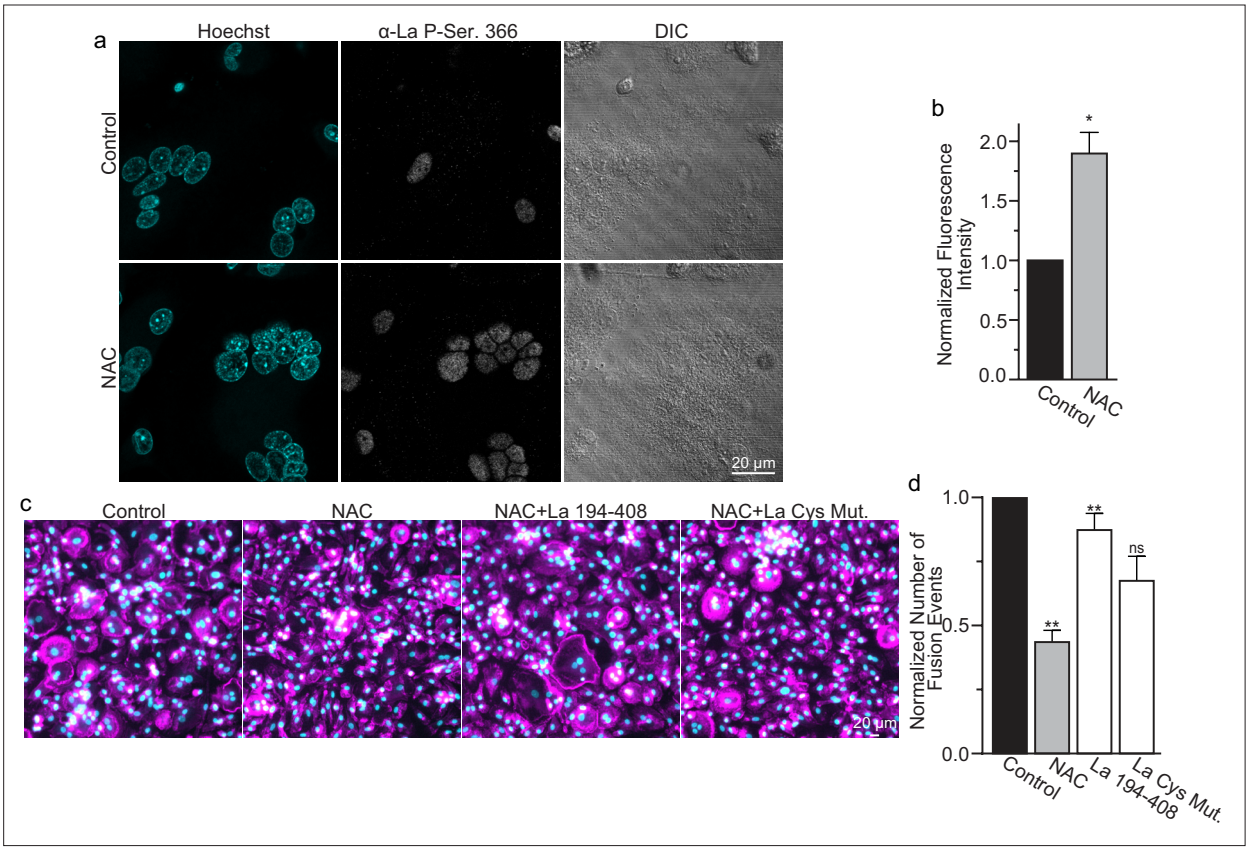

Figure 6. Reactive oxygen species (ROS) signaling promotes dephosphorylation of La and osteoclast fusion by increasing the amounts of oxidized La at the surface of the cells. (**a**) Fluorescence microscopy and differential interference contrast (DIC) images of permeabilized osteoclasts without or with application of 100 mm *N*-acetylcysteine (NAC) (1 hr) stained with an α-La antibody that recognizes La phosphorylated at Ser366. (**b**) Quantification of the staining intensity from (**a**) (n = 3) (p = 0.01). Statistical significance evaluated via paired *t*-test. (**c**) Representative fluorescence images of differentiating osteoclasts in control conditions, conditions where fusion was inhibited via NAC treatment (100 µM NAC added at 2 days post-receptor activator of NF-kappaB ligand [RANKL] application), and conditions where fusion was rescued by the application of recombinant La 194–408 or cysteine mutant La 194–408. (**d**) Quantification of the number of osteoclast fusion events in (**c**) (n = 5) (p = 0.0007, 0.0001, 0.0054, and 0.0352, respectfully). Statistical significance for Control vs NAC or La 190–408 vs La Cys Mutant was evaluated via paired *t*-test (p = 0.0012 and 0.0037, and 0.073, respectively). Statistical significance for NAC vs La 190–408 or La Cys Mutant rescue was evaluated via one-way analysis of variance (ANOVA) with Holm–Sidak correction. * = p < 0.05, ** = <0.01. Data are presented as mean values +/- SEM.

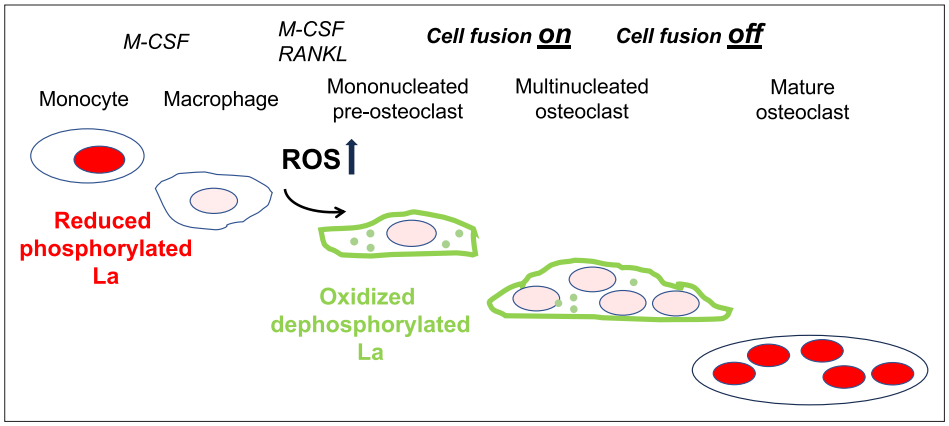

Figure 7. Reactive oxygen species (ROS) signaling induced restructuring of La from reduced to oxidized species triggers La re-localization from nucleus to the surface of differentiating osteoclasts and promotes their fusion and resorptive function. An illustrated depiction of osteoclastogenic differentiation from monocytes to mature bone-resorbing osteoclasts. Machrophage precursors are derived via the macrophage colony-stimulating factor (M-CSF) activation of circulating monocytes. Osteoclastst differentiation is initiated by subsequent application of M-CSF and receptor activator of NF-kappaB ligand (RANKL), which ellicits intracellular ROS production leading to drastic changes in the redox state and localization of La. La transitions from a prodominatly nuclear, reduced species of La in monocytes and macrophages to an oxidized, dephosphorylated species that traffics to and associates with the surface of fusion-competent osteoclasts. When osteoclast arrive at an appropriate size and fusion stops, the mature multinucleated osteoclasts exhibit a predominately nuclear, reduced La species, as is typical of other eukaryotic cells.